

## A DEHYDROGENATION STUDY OF COSMIC CARBON ANALOGUE GRAINS

V. MENNELLA,<sup>1</sup> L. COLANGELI,<sup>1</sup> A. BLANCO,<sup>2</sup> E. BUSSOLETTI,<sup>3</sup> S. FONTI,<sup>2</sup> P. PALUMBO,<sup>4</sup> AND H. C. MERTINS<sup>5</sup>

Received 1994 May 12; accepted 1994 November 8

### ABSTRACT

We present the results of a systematic study of the dehydrogenation produced by thermal annealing of small (average radius  $\langle a \rangle = 5$  nm) hydrogenated amorphous carbon grains. The heat treatment of the particles can be a reasonable simulation of the grain processing active in space as modeled by Hecht (1986) and Sorrell (1990). Extinction measurements both on grains as produced and on samples annealed at fixed temperatures between 250°C and 800°C have been performed in the spectral range 190–800 nm. For some samples the measurements have been extended in the extreme-ultraviolet (EUV) down to 40 nm. The extinction spectra of all the samples analyzed in the EUV are characterized by a band falling around 93 nm. On the other hand, all the samples, but the hydrogenated one, show a peak in the UV region. This feature becomes more and more pronounced and shifts toward longer wavelengths as the annealing temperature increases.

We assign the high- and low-energy bands, respectively, to  $\sigma-\sigma^*$  and  $\pi-\pi^*$  electronic transitions of the  $sp^2$  hybridized carbon clusters forming the grains. We identify these clusters as the major factor responsible for determining the UV extinction properties of our carbon grains. The shift of the peak is interpreted in terms of a dimensional growth of the  $sp^2$  clusters, indicating a progressive graphitization of the samples. The  $\pi-\pi^*$  transition is observed at 259 nm in the samples annealed at 800°C, in close agreement with that observed for graphite (260 nm).

The results of the annealing experiment offer new hints to interpret the circumstellar and interstellar UV extinction bands. In particular, it appears possible to interpret the origin of these features in terms of  $\pi-\pi^*$  electronic transitions in carbonaceous grains.

*Subject headings:* circumstellar matter — dust, extinction — stars: carbon — ultraviolet: ISM

### 1. INTRODUCTION

One of the main problems posed by observations of the interstellar dust is the correct identification of the carriers of the 217.5 nm bump observed in the interstellar extinction curves. The astronomical data obtained so far have shown that the position of the peak is very stable at 217.5 nm, while its width varies from 36 to 77 nm with an average value of 48 nm (Fitzpatrick & Massa 1986; Massa & Savage 1989). Although many models have been proposed to interpret this feature (see, e.g., the review paper by Draine 1989), all of them have difficulties in explaining the observational constraints. Also, the graphite hypothesis, considered a leading model among various authors (i.e., Gilra 1972; Mathis, Rumpl, & Nordsieck 1977; Draine & Lee 1984), fails in accounting for the observed lack of correlation between the bump position and its width (Draine & Malhotra 1993). However, Mathis (1994) considered coatings of graphite grains to interpret the width variations of the 217.5 nm among different sight lines.

Another important feature of the interstellar extinction is the far-ultraviolet (FUV) rise, which is not correlated with the shape and intensity of the bump (Greenberg & Chlewicki 1983; Fitzpatrick & Massa 1988). By analyzing a sample of diffuse medium curves, Greenberg & Chlewicki (1983) found a high

degree of uniformity in the shape of the extinction in the range 130–170 nm. They concluded that the FUV rise is due to pure absorption. This is confirmed by the lack of a rise in the FUV region in the scattering of dust in reflection nebulae (Witt 1989) and in the polarization of radiation from reddened stars (Clayton et al. 1992). On the other hand, Fitzpatrick & Massa (1988) found that two distinct and uncorrelated components are necessary to explain the observed FUV extinction shapes: a curvature component and a linear background. The grains responsible for these two extinction features should belong to separate populations. However, the physical meaning of the FUV curvature has been questioned (Cardelli, Clayton, & Mathis 1989) because there is a priori no reason to extrapolate the linear background to the FUV spectral region. Therefore, at present, the carrier(s) of the FUV extinction remains unidentified.

The UV circumstellar extinction profile is quite different from the interstellar behavior. Sources such as Abell 30 (Greenstein 1981), R CrB and RY Sgr (Hecht et al. 1984), and HD 213985 (Buss, Lamers, & Snow 1989) show a bump falling in the range 230–250 nm. Furthermore, in the case of  $\alpha$  Sco (Snow et al. 1987) and HD 89353 (Buss et al. 1989) the UV peak is lacking.

The different behaviors of interstellar and circumstellar extinctions can be linked to the role of hydrogen in the formation and evolution of carbon grains in space. Hecht (1986) suggested that hydrogenated carbon grains, which condense around carbon-rich stars, may not show the 217.5 nm bump since hydrogen localizes the  $\pi$ -bond and, then, inhibits the collective resonance responsible for this feature. Once the grains are injected in the diffuse medium, they are annealed by exposure to UV radiation, cosmic rays, and shock processes (Sorrell 1990). The consequent dehydrogenation produces a

<sup>1</sup> Osservatorio Astronomico di Capodimonte, via Moiariello 16, I-80131, Napoli, Italy.

<sup>2</sup> Dipartimento di Fisica, Università di Lecce, via per Arnesano, I-73100 Lecce, Italy.

<sup>3</sup> Istituto di Fisica Sperimentale, Istituto Universitario Navale, via A. De Gasperi 5, I-80133 Napoli, Italy.

<sup>4</sup> Dipartimento Ingegneria Aerospaziale, Università degli Studi di Napoli Federico II, Piazzale Tecchio 80, I-80125 Napoli, Italy.

<sup>5</sup> Technical University of Berlin, Institut für Festkörperphysik, Sekr. PN 4-1, Hardenbergstrasse 36, D-1000 Berlin, Germany.

delocalization of the  $\pi$ -bond and the emergence of the peak. In particular, Hecht (1986) identifies the carriers of the 217.5 nm band with small hydrogen-free carbon grains. On the other hand, when the grain formation takes place in circumstellar regions where  $C/H > 1$ , amorphous carbon grains are formed and the UV peak is observed at  $\sim 240$  nm, in agreement with laboratory results (Bussoletti et al. 1987; Colangeli et al. 1993; Muci et al. 1994).

As far as laboratory simulation is concerned, dehydrogenation studies of cosmic carbon analogue grains can play an important role in the previous context. In particular, the analysis of the UV optical properties of hydrogen-rich carbon particles subject to annealing processes can help to interpret astronomical observations and to support theoretical models on an experimental basis. Recently, Blanco et al. (1991, 1993), by means of thermal annealing processes, have shown that the UV spectral properties of hydrogenated amorphous carbon grains are quite sensitive to the hydrogen content. In the present paper we have analyzed similar hydrogenated amorphous carbon grains produced by arc discharge in hydrogen atmosphere. The dependence of the extinction on the annealing temperature in the range 250°C–800°C has been systematically studied. Measurements have been carried out in the spectral range 190–800 nm; for some samples, the extreme-ultraviolet (EUV) spectral range (down to 40 nm) has also been analyzed. In § 2 we report a description of the grain production method and of the setup used to perform the experiments, while the results obtained are described in § 3 and discussed in § 4. Finally, the astrophysical implications of our findings are presented in § 5.

## 2. EXPERIMENTAL SETUP

The experiment on hydrogenated amorphous carbon (hereinafter ACH2) grains was performed simultaneously in the Cosmic Physics Laboratories of Napoli and Lecce with two similar setups. The ACH2 grains were produced by arc discharge between two amorphous carbon electrodes in hydrogen atmosphere, at a pressure of 10 mbar, and collected on UV grade fused silica substrates at a distance of 5 cm from the source. Scanning electron microscopy measurements show that the particles have a spherical shape and are clustered together to form a fluffy structure. The average radius ( $\langle a \rangle = 5$  nm) is very close to that of carbon particles produced in argon atmosphere (Borghesi et al. 1983; Blanco et al. 1991). The thermal annealing of the ACH2 samples was performed at a pressure less than  $10^{-5}$  mbar in a stainless steel cavity maintained in thermal equilibrium by a heater. The temperature of the samples was measured by means of a (NiAl–NiCr) thermocouple and was controlled to better than 1%. The samples were annealed for 3 hr at a fixed temperature,  $T_a$ , in the range 250°C–800°C. For each temperature a freshly produced sample was used. In the following, the samples will be identified with a label that refers to the actual  $T_a$  (see Table 1).

Extinction measurements were performed both before and after each annealing process in the range 190–800 nm by using dispersive double-beam spectrophotometers (Perkin Elmer models Lambda 9 and Lambda 3). To extend the extinction measurements down to 40 nm, we used synchrotron radiation dispersed with a 3 m normal-incidence monochromator as source. This part of the experiment was carried out at the Berliner Elektronenspeicherring-Gesellschaft für synchrotronstrahlung (BESSY). A detailed description of both the experimental apparatus and the technique used is reported

TABLE 1  
UV AND EUV PEAK POSITIONS  
OF THE EXAMINED SAMPLES

Label	$T_a^a$	$\lambda_p^b$ (nm)	$\Lambda_p^c$ (nm)
ACH2 .....	...	...	$93 \pm 2$
AC250 .....	250°C	$194 \pm 2$	$93 \pm 2$
AC325 .....	325	$198 \pm 3$	$95 \pm 2$
AC400 .....	400	$208 \pm 2$	...
AC415 .....	415	$214 \pm 3$	$90 \pm 2$
AC450 .....	450	$216 \pm 4$	...
AC500 .....	500	$230 \pm 4$	...
AC550 .....	550	$241 \pm 2$	...
AC600 .....	600	$246 \pm 2$	...
AC700 .....	700	$252 \pm 4$	...
AC800 .....	800	$259 \pm 4$	...

<sup>a</sup> Annealing temperature.

<sup>b</sup> UV peak position.

<sup>c</sup> EUV peak position.

elsewhere (Colangeli et al. 1993, hereinafter Co93). Here we report only some salient items and briefly describe the approach followed to analyze the samples. We recall that Co93 measured the extinction of carbon grains in the spectral range down to 40 nm by taking advantage of the reflectivity of a gold-coated quartz substrate. The procedure consists of measuring (see Fig. 1 in Co93) (1) the reflectivity,  $R$ , of the gold coating, (2) the intensity,  $I$ , reflected from the substrate after two passages through the dust, and (3) the intensity of the incident beam,  $I_0$ . From these measurements the extinction of the dust can be obtained by means of the relation  $I/I_0 = RT^2$ , where  $T$  denotes the transmission of the dust deposit. The angle formed by the incident beam with the normal direction to the sample is  $5^\circ \pm 2^\circ$ .

In the present measurements we used quartz substrates without the gold coating because preliminary tests showed that the gold coating deteriorated after annealing. This result induced us to choose quartz as substrate. Actually, its reflectivity is comparable with that of the gold in the EUV spectral region, and it does not change in the temperature range considered.

## 3. RESULTS

As already mentioned in the previous section, extinction measurements were performed on samples annealed for 3 hr at various temperatures in the range  $T_a = 250^\circ\text{C}$ – $800^\circ\text{C}$ . For each considered  $T_a$ , annealing processes and spectral measurements were repeated on several samples. Since the results agree quite well, in the following we will refer to the averages of the obtained data. The extinction profiles are shown in Figure 1. We note that, while no peak is evident in the spectrum of grains as produced, all the spectra exhibit a bump in the UV region after annealing. This feature becomes more and more pronounced, and the position of the peak,  $\lambda_p$ , systematically shifts toward longer wavelengths as  $T_a$  increases: starting from 194 nm for the AC250 sample, the peak moves to 259 nm in the case of the AC800 sample. The dependence of the peak position on the annealing temperature is shown in Figure 2. Three distinct behaviors can be identified for  $\lambda_p$  versus  $T_a$ : (1) a slow variation at low temperatures, (2) a rapid increase in the range  $400^\circ\text{C}$ – $600^\circ\text{C}$ , and (3) again a slow variation for  $T_a \geq 600^\circ\text{C}$ .

For the samples annealed at  $T_a < 415^\circ\text{C}$  the peak position is very close to the shortest wavelength limit of our spectrophotometers (190 nm) (see Fig. 1 and Table 1). Therefore, we

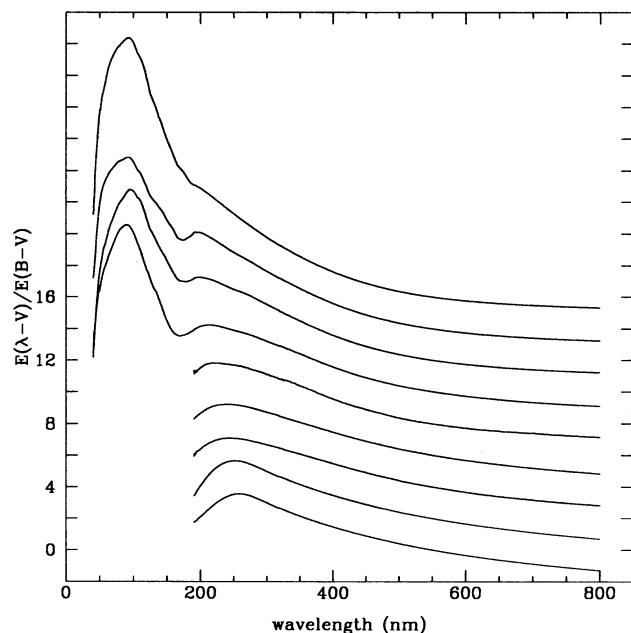


FIG. 1.—Extinction spectra of the analyzed samples. From top to bottom, the spectra in the figure refer to the ACH2, AC250, AC325, AC415, AC500, AC550, AC600, AC700, and AC800 samples, respectively. The ordinate scale refers to AC800; all the other spectra are shifted with respect to each other by two units. The uncertainty on the wavelength is about  $\pm 0.5$  nm, while the random errors on the normalized extinction data are smaller than 5%.

extended the spectrophotometric measurements on AC250, AC325, and AC415 samples to shorter wavelengths by means of the BESSY facility. We also measured the extinction of ACH2 and amorphous carbon grains produced by arc discharge in Ar atmosphere (ACAr). Since these samples were not annealed, we were able to perform measurements on grains

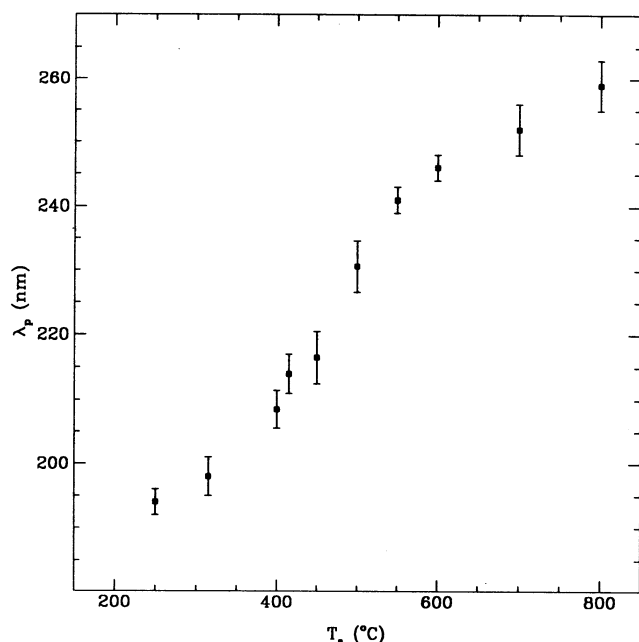


FIG. 2.—UV peak position of hydrogenated carbon grains annealed for 3 hr as a function of the annealing temperature. The error bars represent the uncertainties determined from repeated experiments on different samples.

deposited both on gold-coated and on bare quartz substrates. This allowed us to check any possible influence of the substrate on the extinction of the dust. No differences were noticed, within the experimental errors, between the extinction spectra obtained in the two cases. Moreover, the results obtained for ACH2 and ACHAr agree with those reported in Co93. These elements confirm the validity of our technique to derive the extinction in the EUV and allow us to be confident in the extinction obtained for the annealed carbons.

As one can see in Figure 1, all the samples analyzed in the EUV region are characterized by a minimum and a second bump in the extinction profile falling around 170 and 93 nm, respectively (see Table 1). Unlike the bump at lower energy, the peak position of the EUV feature does not vary with  $T_a$  up to 415°C. In order to investigate the behavior of the peak at higher temperatures, measurements are scheduled for the next shift at the BESSY facility. However, due to the different origin of the two resonances (see next section), we expect a different behavior of the two features at higher annealing temperatures as well.

#### 4. DISCUSSION

The results obtained in our experiment show that important modifications take place in the spectra of hydrogenated amorphous carbon grains due to annealing (see Figs. 1 and 2). In fact, the UV spectrum of ACH2 is featureless beyond 190 nm, while a peak appears after annealing. Its position and strength depend on the temperature  $T_a$ . In agreement with Blanco et al. (1991, 1993) the spectral changes can be interpreted in terms of dehydrogenation of the samples.

This conclusion is corroborated by measurements of the hydrogen content for two of our samples (ACH2 and AC400) performed by Archuleta, Devlin, & Trkula (1993). Mass-calibrated samples were burned in a small sealed metal container in oxygen atmosphere. Then, the heat capacity of the gases produced by the burned samples was determined as a function of the temperature. By measuring the heat capacity in the range 80°C–100°C due to the water evaporation, the mass of water and, then, the mass of hydrogen were determined with respect to the total mass of the sample. The mass ratios obtained for ACH2 and AC400 samples are 0.049 and 0.018, respectively. The accuracy of these values is  $\sim 10\%$ . The corresponding H/C atom ratios are 0.62 and 0.22. These values were obtained under the hypothesis that the samples contain only hydrogen and carbon.

From our results (see Fig. 2) it appears that hydrogenated amorphous carbon grains show the faster  $\lambda_p$  variation, as a function of  $T_a$ , in the same temperature range (400°C–600°C) where a-C:H (hydrogenated amorphous carbon films) presents a complete hydrogen loss and structural variations during heat treatments. In particular, Fink et al. (1984) observed a delocalization of  $\pi$ -electrons between 400°C and 600°C. Similarly, Dischler, Bubenzer, & Koidl (1983) found that the  $sp^2$  fraction in their a-C:H begins to increase at 400°C and it reaches almost 100% at 600°C. Finally, Smith (1984) indicates 450°C as the temperature at which the most rapid hydrogen effusion occurs.

One of the most important effects of hydrogen loss from carbon grains is a rearrangement of the electronic structure (Robertson 1986). The presence of hydrogen in the grains promotes the formation of  $sp^3$  bonds with a consequent localization of  $\pi$  and  $\pi^*$  electronic bands. Therefore, a collective excitation of  $\pi$ -electrons is not possible in hydrogenated



carbons. Once the hydrogen is removed during the annealing, the bonding becomes progressively more unsaturated: the portion of  $sp^2$  delocalized bonds rises and the  $\pi$ -plasmon can become active.

At this point it is important to recall that electron energy loss spectra (EELS) of a-C:H obtained by Fink et al. (1984) show no evidence for the  $\pi$ -plasmon, although the higher energy  $\sigma + \pi$  plasmon near 23 eV is present. Upon annealing at 600°C the  $\pi$ -plasmon at 6 eV (207 nm) appears, while the  $\sigma + \pi$  plasmon slightly decreases in energy. Fink et al. (1984) also found that the imaginary part of the dielectric function,  $\epsilon_2$ , of a-C:H is characterized by a  $\sigma$ - $\sigma^*$  transition falling at  $\sim 13$  eV and by a  $\pi$ - $\pi^*$  transition. The latter is formed by the graphitic transition (at  $\sim 4$  eV, i.e., 310 nm), arising from  $\pi$ -electrons delocalized on several aromatic rings, and by a feature at  $\sim 6.5$  eV (191 nm) attributed to benzene rings. However, after annealing, the 6.5 eV transition disappears and the graphitic band becomes more and more pronounced. The  $\pi$  and  $\sigma + \pi$  plasmons have also been observed, respectively, at  $\sim 6$  and  $\sim 20$  eV in the EELS spectra of coals (Papoular et al. 1993).

In the light of the above-reported discussion we can interpret our experimental results on hydrogenated amorphous carbon grains: the spectral changes observed as a function of the annealing temperature can be explained in terms of structural modifications of the particles. We attribute the high energy around 93 nm (13 eV) to  $\sigma$ - $\sigma^*$  transitions rather than to the  $\sigma + \pi$  plasmon, since the energy of this transition is very close to that observed in graphite, a-C:H, and a-C (amorphous carbon films), while the  $\sigma + \pi$  plasmon has been observed in the energy range from 20 to 25 eV (see Robertson 1986). Moreover, we assign the lower energy extinction peak to a  $\pi$ - $\pi^*$  interband transition of  $sp^2$  clusters forming the grains. The previous assignment is supported by theoretical studies on the electronic properties of amorphous carbons. In fact, Robertson (1986) and Robertson & O'Reilly (1987) have shown that the most stable arrangement of  $sp^2$  sites is in compact clusters of fused sixfold rings, i.e., graphitic layers.

The shift of the peak as a function of  $T_a$  can be interpreted in terms of a dimensional growth of the  $sp^2$  clusters. In the case of the AC250 sample, the peak position at 194 nm is very close to that measured for a-C:H (191 nm); this indicates that the clusters in the grains are mainly formed by only a few benzene rings. On the other hand, for the AC800 sample the peak position ( $\lambda_p = 259$  nm) coincides with that (260 nm) observed in the transmission spectrum of ultrathin flakes of single graphite crystals (Ergun & McCartney 1963; Marchand 1987). Even if the width of the band is broader than that of graphite, its position indicates that graphitic clusters have grown.

The trend of  $\lambda_p$  as a function of  $T_a$  observed in our experiment can be considered evidence against the attribution of this peak to a  $\pi$ -plasmon. The  $\lambda_p$  shift toward lower energies is opposite to that expected for a plasmon. We recall that the energy of the plasmon is

$$E_p = (4\pi e^2 \hbar^2 N n_{\text{eff}} / m)^{1/2},$$

where  $\hbar$  is the reduced Planck constant,  $e$  and  $m$  are, respectively, the charge and the mass of the electron,  $N$  is the number of C atoms per unit volume, and  $n_{\text{eff}}$  is the effective number of electrons per atom which have contributed to the excitations. As the plasmon energy is proportional to  $(N n_{\text{eff}})^{1/2}$ , the observed shift of the peak toward lower energy would imply a decrease of  $N$  and/or  $n_{\text{eff}}$ , if the band observed in the spectra

were due to a plasmon resonance in our grains. Actually, even if we did not measure the density of our samples, we recall that a 21% density increase for a-C:H annealed at 750°C was observed by Smith (1984). Furthermore, the annealing of the samples should produce an increase of  $sp^2$  sites and, therefore, of  $n_{\text{eff}}$  for  $\pi$ -electrons. An increase of  $n_{\text{eff}}$ , going from a-C:H to more graphitic a-C is indeed reported by Robertson (1991).

We conclude that the two peaks present in the analyzed spectra are due to electronic transitions rather than to collective excitations. This modifies the interpretation of the two features given so far. A more general conclusion is that the  $sp^2$  clusters forming our grains are the most responsible for the observed UV spectral properties. In order to confirm this hypothesis other complementary measurements about the morphology and the structure of our grains are needed; they will be the subject of a forthcoming paper (Mennella et al. 1995).

## 5. ASTROPHYSICAL IMPLICATIONS

The thermal annealing considered in the present work can be a reasonable simulation of the carbon grain processing active in space, as modeled by Hecht (1986) and Sorrell (1990). We recall that when UV photons are absorbed by hydrogenated carbon particles, the grains can be heated up to temperatures high enough to eject H atoms before they chemisorb again into CH bonds (Sorrell 1990). Although in the diffuse medium the flux of cosmic rays is smaller than that of UV photons, a heating process could also be activated by cosmic rays. According to the laboratory results obtained by Strazzulla & Baratta (1992), the interaction of ions with grains would produce a hot track in the solid so that hydrogen loss can occur. Thus, the heat treatment of grains in the laboratory can be, in a first approximation, a valid tool to study the origin of spectral changes of interstellar carbonaceous grains due to annealing.

Another point that we want to stress is that the size of the grains analyzed in this work ( $\langle a \rangle = 5$  nm) agrees with that of the hydrogen-free carbon grains proposed by Hecht (1986) as carriers of the 217.5 nm feature. Moreover, Sorrell (1990), by studying UV irradiation of hydrogenated carbon, concluded that only Rayleigh-size graphitic carbon grains can be formed in the interstellar medium by UV annealing.

Actually, our grains are linked in a fluffy structure, while particles are expected to be isolated in space, so that spectral modifications produced by clustering could affect the results, in particular the bump profile (Huffman 1989; Wright 1989). Nevertheless, we believe that the spectral variations and, in particular, the peak shift we observe are due to structural variations rather than to interactions with nearby grains. This conclusion is supported by morphological analyses of the samples annealed at different temperatures performed by means of scanning and transmission electron microscopy: while variations of the optical properties are present, no difference has been revealed in the size and clustering degree of the grains (Blanco et al. 1993; Mennella et al. 1995).

The models outlined so far to fit the profile of the interstellar bump have used the optical constants of bulk graphite and have assumed that the  $\pi$ -electronic resonance can be treated as surface plasmon (Gilra 1972; Hecht 1986; Draine 1989; Sorrell 1990). The presence of large graphite grains in space has been questioned because it is difficult to form such ordered materials around carbon stars or by annealing of amorphous carbon grains in the interstellar medium (Bussoletti et al. 1987; Mathis

& Whiffen 1989). However, Rayleigh-size graphitic grains, produced by annealing processes in the interstellar medium, have been proposed as carriers of the extinction bump. The results of the present experiment indicate that we have been able to produce cosmic carbon analogue grains whose fundamental optical properties ( $\pi$ - $\pi^*$  and  $\sigma$ - $\sigma^*$  transitions) are quite similar to those of graphite. The structure of the grains is, however, far from the perfect crystal, at least for annealing temperatures up to 800°C. They should be composed of  $sp^2$  clusters forming a disordered structure. Therefore, the use of optical constants of graphite to fit the interstellar bump should be considered only a first approximation of the actual conditions.

The limit of the graphite hypothesis in explaining the observational constraints has been pointed out by Draine & Malhotra (1993). These authors concluded that the observed variations in width of the interstellar bump cannot be explained by changes in graphite grain size, shape, clumping, or coating, but they must instead be due to changes in the dielectric properties of the graphitic material forming the grains. According to the same authors, the modifications of the optical properties can be due to (1) impurities (particularly hydrogen), (2) variations in the degree of crystallinity, or (3) surface effects. In the light of our experimental results we believe that the first two items are strongly correlated. In fact, hydrogen, by promoting  $sp^3$  hybridization of carbon atoms, regulates the dimensions of the  $sp^2$  clusters and, then, the electronic structure of the carbonaceous grains.

The wavelength shift of the UV peak observed in our measurements (see Fig. 2) allows us to identify carbonaceous structures able to reproduce the position of the interstellar bump. Similarly, Papoular et al. (1993), by studying coals with different ranks, concluded that only one kind (La Mure) of these carbonaceous materials is able to fit reasonably the interstellar bump profile. These authors exclude plasmon resonance as the origin of the measured band. Then, both for carbon grains and for coals it could be unnecessary to invoke plasmon resonances to interpret the UV extinction band. However this approach requires peculiar structural properties for the carriers of the 217.5 nm bump.

At present we do not see any compelling reason why this specific kind of material should be dominant in the interstellar

medium. More detailed studies are needed to take into account the actual physical conditions present in space. In addition, the grains responsible for the 217.5 nm bump should be extremely resilient. There is considerable evidence that they can suffer modifications giving rise to a broad or narrow feature depending on the evolution and the environmental conditions (Fitzpatrick & Massa 1986; Cardelli & Savage 1988). This behavior has been modeled by either coated graphite grains (Mathis 1994) or hydrogenated graphite particles (Hecht 1986). As mentioned above, our experiment is consistent with the approach proposed by Hecht, even if in the present work we have only considered the effects produced by annealing. The influence of other parameters, such as  $sp^2$  cluster size distribution, impurities, and surface effects, should be accounted for in order to explain the bump profile variations observed in different astronomical environments.

As far as the circumstellar bump is concerned, we note a good match of both peak position and profile with amorphous carbon grains produced in Ar atmosphere (Muci et al. 1994). The same agreement can be obtained with the hydrogenated carbon grains annealed at 600°C studied in the present work. We recall that 600°C is the typical temperature at which a complete hydrogen loss is achieved. These considerations seem to imply that dehydrogenated carbon grains are good candidates to simulate circumstellar observations. We tend to attribute the bump to a  $\pi$ - $\pi^*$  electronic transition rather than to a plasmon resonance.

In conclusion, the discussion reported above opens a new line of interpretation of the nature of the interstellar and circumstellar bumps. Further laboratory experiments and theoretical simulations have to be carried out in the future to try to disclose the remaining mystery of the ubiquitous 217.5 nm interstellar bump.

T. Archuleta, D. Devlin, and M. Trkula are warmly thanked for the hydrogen content measurements performed at Los Alamos National Laboratory. We thank S. Inarta, N. Staiano, and E. Zona for their technical assistance. This work has been supported by the European Community Large Scale Installations Program contract GE 1-0018-D(b) and ASI, CNR, and MURST research contracts.

## REFERENCES

- Archuleta, T., Devlin, D., & Trkula, M. 1993, private communication  
 Blanco, A., Bussoletti, E., Colangeli, L., Fonti, S., Mennella, V., & Stephens, J. R. 1993, *ApJ*, 406, 739  
 Blanco, A., Bussoletti, E., Colangeli, L., Fonti, S., & Stephens, J. R. 1991, *ApJ*, 382, L97  
 Borghesi, A., Bussoletti, E., Colangeli, L., Minafra, A., & Rubini, F. 1983, *Infrared Phys.*, 23, 85  
 Buss, R. H., Lamers, H., & Snow, T. P. 1989, *ApJ*, 347, 977  
 Bussoletti, E., Colangeli, L., Borghesi, A., & Orofino, V. 1987, *A&AS*, 70, 257  
 Cardelli, J. A., Clayton, G. C., & Mathis, J. S. 1989, *ApJ*, 345, 245  
 Cardelli, J. A., & Savage, B. D. 1988, *ApJ*, 325, 864  
 Clayton, G. C., et al. 1992, *ApJ*, 385, L53  
 Colangeli, L., Mennella, V., Blanco, A., Fonti, S., Bussoletti, E., Gumlich, H. E., Mertins, H. C., & Jung, C. 1993, *ApJ*, 418, 435 (Co93)  
 Dischler, B., Bubenzer, A., & Koidl, P. 1983, *Solid State Comm.*, 48, 105  
 Draine, B. T. 1989, in *Interstellar Dust*, ed. L. J. Allamandola & A. G. G. M. Tielens (Dordrecht: Kluwer), 313  
 Draine, B. T., & Lee, H. M. 1984, *ApJ*, 285, 89  
 Draine, B. T., & Malhotra, S. 1993, *ApJ*, 414, 632  
 Ergun, S., & McCartney, J. T. 1963, in *Proc. 5th Conf. on Carbon* (Oxford: Pergamon), 2, 167  
 Fink, J., Müller-Heinzerling, T., Pflüger, J., Scheeler, B., Dischler, B., Koidl, P., Bubenzer, A., & Sah, R. E. 1984, *Phys. Rev. B*, 30, 4713  
 Fitzpatrick, E. L., & Massa, D. 1986, *ApJ*, 307, 286  
 ———. 1988, *ApJ*, 328, 734  
 Gilra, D. P. 1972, in *Scientific Results from the Orbiting Astronomical Observatory OAO 2*, ed. A. D. Code (NASA SP-310)  
 Greenberg, J. M., & Chlewicki, G. 1983, *ApJ*, 272, 563  
 Greenstein, J. L. 1981, *ApJ*, 245, 124  
 Hecht, J. H. 1986, *ApJ*, 305, 817  
 Hecht, J. H., Holm, A. V., Donn, B., & Wu, C. C. 1984, *ApJ*, 280, 228  
 Huffman, D. R. 1989, in *Interstellar Dust*, ed. L. J. Allamandola & A. G. G. M. Tielens (Dordrecht: Kluwer), 329  
 Marchand, A. 1987, in *Polycyclic Aromatic Hydrocarbons and Astrophysics*, ed. A. Leger, L. d'Hendecourt, & N. Boccaro (Dordrecht: Reidel), 31  
 Massa, D., & Savage, B. D. 1989, in *Interstellar Dust*, ed. L. J. Allamandola & A. G. G. M. Tielens (Dordrecht: Kluwer), 3  
 Mathis, J. S. 1994, *ApJ*, 422, 176  
 Mathis, J. S., Rimpl, W., & Nordsieck, K. H. 1977, *ApJ*, 217, 425  
 Mathis, J. S., & Whiffen, G. 1989, *ApJ*, 341, 808  
 Mennella, V., Colangeli, L., Bussoletti, E., Monaco, G., Palumbo, P., & Rotundi, A. 1995, *ApJ*, submitted  
 Muci, A. M., Blanco, A., Fonti, S., & Orofino, V. 1994, *ApJ*, 436, 831  
 Papoular, R., Breton, J., Gensterblum, G., Nenner, I., Papoular, R. J., & Pireaux, J. J. 1993, *A&A*, 270, L5  
 Robertson, J. 1986, *Adv. Phys.*, 35, 317  
 ———. 1991, *Prog. Solid State Chem.*, 21, 199  
 Robertson, J., & O'Reilly, E. P. 1987, *Phys. Rev. B*, 35, 2946  
 Smith, F. S. J. 1984, *Appl. Phys.*, 55, 764  
 Snow, T. P., Buss, R. H., Gilra, D. P., & Swings, J. P. 1987, *ApJ*, 321, 921  
 Sorrell, W. H. 1990, *MNRAS*, 243, 570  
 Strazzulla, G., & Baratta, G. A. 1992, *A&A*, 266, 434  
 Witt, A. N. 1989, in *Interstellar Dust*, ed. L. J. Allamandola & A. G. G. M. Tielens (Dordrecht: Kluwer), 87  
 Wright, E. L. 1989, *ApJ*, 346, L89